Polymer Chemistry

Accepted Manuscript

This article can be cited before page numbers have been issued, to do this please use: T. Cowen, K. Karim and S. Piletsky, *Polym. Chem.*, 2018, DOI: 10.1039/C8PY00829A.

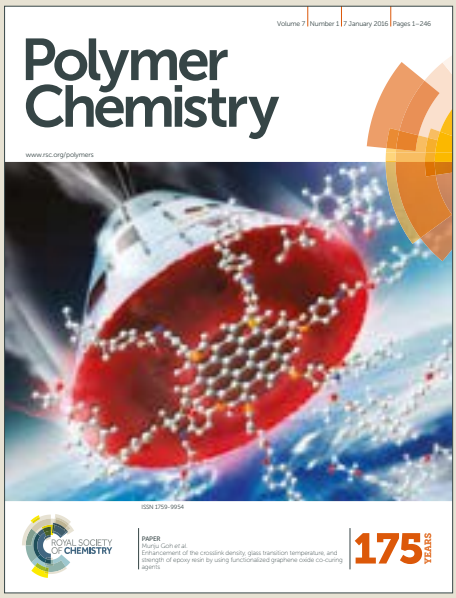

ROYAL SOCIETY OF CHEMISTRY

rsc.li/polymers

View Article Online
DOI: 10.1039/C8PY00829A

Journal Name

ARTICLE

Solubility and size of polymer nanoparticles

Todd Cowen,*[a] Kal Karim [a] and Sergey A. Piletsky [a]

Received 00th January 20xx,
Accepted 00th January 20xx

DOI: 10.1039/x0xx00000x

www.rsc.org/

The solubility of polymer nanoparticles is a complex phenomenon dependent on solvent-solute and solute-solute interactions. Contrary to phase separation in standard polymerization reactions, which is well established research area, the relationship between the solubility of polymer nanoparticles and the resulting diameter of the nanoparticles has been largely overlooked. Herein we demonstrate that the absolute size of polymer nanoparticles can be predicted (and controlled) by varying the relevant parameters of the polymerization conditions that influence the solubility and Flory parameter, $\chi_{s,p}$. The position of the spinodal, associated with a given $\chi_{s,p}$ equivalent and determined with a simple thermodynamic model, allows an absolute value, $\Delta\chi_{spinodal}$, to be applied in predicting polymer dimensions. The hydrodynamic diameter of particles at the primarily observed fraction was found to be dependent on D(nm) = $-74\Delta\chi_{spinodal}$ + 367 nm, where $\Delta\chi_{spinodal}$ must be positive for successful separation. Variation with total polymer fraction over a limited range can also be observed to follow a trend of approximately D(nm) = $173\ln[(xN)^2 10^{-36}/\Delta\chi_{spinodal}]$ – 193 nm, thus giving a more general description of polymerization. We also assert the importance of separating spinodal-character phase separation from binodal-character phase separation in polymer nanoparticle synthesis. To the best of our knowledge this is the first successful Flory-Huggins based thermodynamic model of polymer nanoparticles, and should provide a useful guide to predictive design of future nanomaterials.

Introduction

Solubility is often referenced in simplistic absolute terms, a given particle being referred to as 'soluble' or 'insoluble' in a given solvent. Solubility however exists as a spectrum, and will dependent on the strength of interactions between particles. In common solution theory, an approximation can be made that the closer in chemical nature the two components, the more readily the two will mix to form a single phase. This is obvious from the example of dissolving a liquid in that same liquid; water mixed into water makes water.

The cohesive energy of a material is the total potential energy of intermolecular interaction between components of that materials, given relative to the (negligible) intermolecular potential energy of the vaporized material.[1,2] The cohesive energy density (the cohesive energy per volume of material) is proportional to the enthalpy of vaporization for many common applications.[3] Considering the above example of water added to water, the energy required for intermolecular bond breaking, to accommodate the additional water, will be equal to the energy released on bond formation, and the total energy change between the individual molecules is zero.

With different materials, as with a solute and solvent, the cohesive energy of each will be different, as will the energy released on bonding between solute and solvent relative to that of solvent-solvent and solute-solute interactions. In this context it is more useful to consider each component as having a solubility parameter, δ, equal to the square root of the cohesive energy, with the solubility of one substance in another being inversely proportional to the difference in solubility parameter: 'like dissolves like', due to the similarities of the interactions.[1,2,4,5]

During the process of a chemical reaction the solubility of the solutes changes from that of the reactants to that of the product; in polymerization this change may be large, but it is the result of many small changes in solubility associated with forming the polymer. In the case of polymer nanoparticles, this basis has many consequences which have not been examined in detail previously, most importantly in the control of nanoparticle diameter.

This control of dimensions and other properties will be of particular importance to those developing nanoparticles for drug delivery and diagnostics, an area that has attracted substantial interest.[6-12] Increased attention to the specifics of nanoparticle efficacy, toxicity and preparation for *in vivo* applications are more recent however, an obviously encouraging shift being observable from plausibility to practicality.[13-15] Cellular uptake of nanoparticles, their systemic circulation and excretion, depend on the particles physical structure and chemical composition. The dimensions of nanoparticles intended for biological application is particularly

[a] Department of Chemistry, University of Leicester, Leicester, LE1 7RH, UK. E-mail: tc203@leicester.ac.uk

† Electronic Supplementary Information (ESI) available: Full DLS data as Excel files. Appendix 1 gives measurements at the standard polymer fraction with water-THF variation, Appendix 2 contains variation in polymer fraction and alternate systems. See DOI: 10.1039/x0xx00000x

View Article Online
DOI: 10.1039/C8PY00829A

important influencing, particle diameter being inversely proportional to cellular uptake, but also toxicity and nonspecific cellular absorption.[16,17]

The optimal particle radius for cellular uptake is approximately 30-50 nm for various types of nanoparticles and cells, smaller particles being required to cluster before absorption became energetically favorable, while particles larger than 50 nm are hindered by the greater time required for membrane wrapping.[18-21] Other examples however show that a greater total mass of polymer absorbed is observed for particles of 125 nm,[22] and smaller particles cause an increase in reactive oxygen species (ROSs) generation, toxicity and cell death.[22,23] This is likely related to the greater surface area associated with having a large number of smaller particles. Regardless, an upper limit of 200 nm has been suggested for particles applied *in vivo* to allow effective removal from the circulatory system and avoid accumulation in the spleen.[10,14,24,25] Doubtless the preferred particle diameter will vary with the application, but an effective basis for the control of dimensions is necessary to appropriately respond to such requirements.

The general trends between the diameter of polymer nanoparticles and solubility of polymer components in a particular solvent during their synthesis has been noted previously, but in the absence of thermodynamic considerations predictive design of nanoparticles has so far was unsuccessful.[26-29] Herein we develop a particle model of classical Flory-Huggins theory (FHT) and demonstrate the significance of the spinodal condition in synthesis of nanoparticles. This model allows prediction and most importantly control of dimensions of synthesized polymer nanoparticles providing a relationship between polymer dimensions, system fraction and solvent interactions.

Experimental

Materials and methods

The reaction conditions used here are adapted from that which has been widely used in the preparation of polymer nanoparticles.[30] *N*-isopropylacrylamide (NiPAm), *N*,*N*'-methylenebis(acrylamide) (Bis), ammonium persulfate (APS) and *N*,*N*,*N*',*N*'-tetramethylethylenediamine (TEMED) were obtained from Sigma-Aldrich, *N*-*tert*-butylacrylamide (TBAm) and acrylic acid (AAc) from Acros and streptomycin sulfate from Amresco. Peak mean hydrodynamic diameters were analyzed by DLS using a Zetasizer Nano S (Malvern). The collected DLS data are given in the Appendices.

Synthesis

NiPAm (19.5 mg, 0.193 mmol), TBAm (16.5 mg, 0.143 mmol), Bis (1 mg, 6.486 µmol) and AAc (1.1 µl, 16.02 µmol) were dissolved with or without the nucleant streptomycin sulfate (2.4 mg, 3.245 µmol). Solvents were varied by percentage volume in 5 % increments, giving solvents 100 %-50 % water with the remainder the relevant solvent. Nitrogen was passed through each solution for 25 minutes before initiation with an aqueous solution of APS (15 mg, 65.73 µmol) and TEMED (15 µl, 0.100 mmol). Each mixture was then topped to 50 ml total volume to give the appropriate solvent ratio and briefly degassed again with nitrogen before being left to incubate for approximately 22 hours.[31] The reactions were quenched by passing oxygen gas through each flask for 25 minutes. Variations on this composition involved scaling all components by a common value.

Particle hydrodynamic diameters were analyzed by DLS, the appropriate density, viscosity and refractive index for each solvent mixture was calibrated using previously published empirical data.[32-35] For DLS analysis all data for each conditions was combined and ordered by polydispersity index (PdI); measurements with count rate values (kcps) below 1000 being rejected. The majority of measurements used in the final analysis displayed a polydispersity index below 0.06 (difficulties obtaining low-PdI, high-count measurements with water and water-methanol mixtures required a greater tolerance).

Results and discussion

Solubility parameters

Existing literature data and preliminary experiments suggested that the relative solubility of nanoparticles may correlate with diameter, and that the solubility may be approximated with the use of solubility parameter theory. A molecule may be described in terms of three intermolecular interaction components: dispersive forces, δ_d, polarity, δ_p, and hydrogen bonding, δ_h. Combined together these values give the solubility parameter of the substance, δ, representing the coordinates of the material's solubility in terms of δ_d, δ_p and δ_h. The three interaction components can be obtained directly from the literature for common materials or calculated based on group contribution, in which values for the molecule are approximated based on the number of methyl, methanediyl, methylene, etc. groups. Here this approach is used to build a minimum statistical polymer unit (MSPU), the cross-linked equivalent of the repeat unit based on the initial monomer ratio, the number of each chemical group calculated from the number of that group in the initial monomer composition (accounting for the structure post-polymerization).[36] Group contribution tables vary with the method of treatment, and likely the two most accurate methods are those of Hoftyer-Van Krevelen and Hoy.[37] After some initial analysis, the Hoy method was found to be more appropriate for the materials studied.

Hoy's system begins with group contributions for F_t, the molar attraction function (the cohesive energy per volume), F_p, the polar component of the molar attraction function, V, the molar volume of the MSPU, and $\Delta_T^{(P)}$, a correction for non-ideality.[37] Each is calculated from the sum of the values given for each group i present in the MSPU:

$$F_t = \sum_i n_i F_{t,i} \quad \text{Eq. 1a}$$

$$F_p = \sum_i n_i F_{p,i} \quad \text{Eq. 1b}$$

View Article Online
DOI: 10.1039/C8PY00829A

$$V = \sum_i n_i V_i \quad \text{Eq. 1c}$$

$$\Delta_T^{(P)} = \sum_i n_i \Delta_{T,i}^{(P)} \quad \text{Eq. 1d}$$

There are also two auxiliary equations for polymers, $\alpha^{(P)} = 777\Delta_T^{(P)}/V$ and $\bar{n} = 0.5/\Delta_T^{(P)}$, and the base value $B = 277$. The expressions for the solubility parameter components are then given in Equations 2a-d:[38]

$$\delta_t = \frac{F_t + B/\bar{n}}{V} \quad \text{Eq. 2a}$$

$$\delta_p = \delta_t \left(\frac{1}{\alpha^{(P)}} \frac{F_p}{F_t + B/\bar{n}}\right)^{\frac{1}{2}} \quad \text{Eq. 2b}$$

$$\delta_h = \delta_t \left(\frac{\alpha^{(P)} - 1}{\alpha^{(P)}}\right)^{\frac{1}{2}} \quad \text{Eq. 2c}$$

$$\delta_d = \left(\delta_t^2 - \delta_p^2 - \delta_h^2\right)^{\frac{1}{2}} \quad \text{Eq. 2d}$$

These solubility parameter components can then be used to determine the relative solubility of the substance in another substance by the principle that 'like dissolves like' with Equation 3:

$$\Delta\delta = \left(\left(\delta_{d,p} - \delta_{d,s}\right)^2 + \left(\delta_{p,p} - \delta_{p,s}\right)^2 + \left(\delta_{h,p} - \delta_{h,s}\right)^2\right)^{\frac{1}{2}}$$

Eq. 3

Or often

$$R_{s,p} = \left(4\left(\delta_{d,p} - \delta_{d,s}\right)^2 + \left(\delta_{p,p} - \delta_{p,s}\right)^2 + \left(\delta_{h,p} - \delta_{h,s}\right)^2\right)^{\frac{1}{2}}$$

Eq. 4

Where $R_{s,p}$ is a modified form of $\Delta\delta$ representing the 'distance' between the solubilities of two substances when plotted in three dimensions, with the constant 4 more accurately representing the dispersion forces.[39]

A greater value of $\Delta\delta$ or $R_{s,p}$ therefore indicates reduced affinity of the solute for the solvent, which in the example of precipitation polymerization is equivalent to smaller particles. A further modification includes the introduction of the Flory interaction parameter, $\chi_{s,p}$, which can be approximated using Equation 5:

$$\chi_{s,p} = \frac{1}{k_B T}\left(\varepsilon_{s,p} - \frac{1}{2}\left(\varepsilon_{p,p} + \varepsilon_{s,s}\right)\right) = \frac{V_s R_{s,p}^2}{RT} \quad \text{Eq. 5}$$

The Flory parameter is therefore a measure of the relative affinity of the polymer unit to the solvent, with smaller values indicating greater $\varepsilon_{p,s}$ interactions, and so increased preference for miscibility. $\chi_{s,p}$ can also be used in approximations of the system's entropy and Gibbs free energy, making it useful for further theoretical development.

The data in Table 1 shows calculated values of $R_{s,p}$ ('distance in solubility'), $\chi_{s,p}$ and measured hydrodynamic diameters of polymer nanoparticles synthesized in solution of water and tetrahydrofuran mixed in different ratios. Nanoparticles were prepared based on a protocol used in the synthesis of polymers tested in vivo.[30,40,41] Values of V_s, δ_d, δ_p, and δ_h for these mixtures were calculated from known values of pure solvents using the equation: $\delta_{i,j} = \Sigma\ \phi_i\ \delta_{i,j}$. From results obtained it can be concluded that only the Flory parameter yields successful prediction of fluctuation of diameter of polymer nanoparticles prepared in solution of different polarity.

Table 1 Relationship between solubility parameter components, $R_{s,p}$, $\chi_{s,p}$, and observed hydrodynamic diameter of polymer nanoparticles. Only $\chi_{s,p}$ is seen to effectively predict the initial reduction in polymer diameter with increasing THF content.

Water vol% of solvent	V_s, $cm^3\ mol^{-1}$	$R_{s,p}$	$\chi_{s,p}$	Diameter, nm
100	18.00	32.242	7.5526	209 ± 4
95	21.19	30.470	7.941	196 ± 19
90	24.37	28.700	8.102	178 ± 9
85	27.56	26.936	8.071	163 ± 18
80	30.74	25.175	7.864	190 ± 16
75	33.93	23.421	7.512	223 ± 13
70	37.11	21.675	7.037	280 ± 34
65	40.30	19.936	6.465	297 ± 12
60	43.48	18.213	5.821	335

A simple model for calculation of Gibbs energy of mixing polymers and solvents

In FHT the thermodynamics of mixing is constructed so as to account for the many configurations that a polymer chain may take. The polymeric particles formed here however can be better represented by spheres, interchangeable by rotation, and with each other. This requires an alternative model, but the general methodology and terminology of Flory will be followed.

The system is assumed to be a 3D lattice of cells, each cell being the volume of the MSPU, with solvents being represented as clusters of individual molecules amounting to the volume of one cell.[42] The total volume is given by n_0, total number of polymer particles by N, total number of MSPU units per particle (used in analogy to both the polymer volume and degree of polymerization) being x, and the total number of solvent clusters being given by n; thus $n_0 = n + xN$.

A simple model of the entropy of mixing can be applied, as given in Equation 6:

$$\Delta S_m = -k_B\left[n \ln\left(\frac{n}{n_0}\right) + N \ln\left(\frac{xN}{v}\right)\right] \quad \text{Eq. 6}$$

Where v is the volume that can be occupied by the central MSPU of the particle:

$$v = n_0 - \left(\frac{3x}{4\pi}\right)^{\frac{1}{3}} 6\left(\sqrt[3]{n_0}\right)^2 \quad \text{Eq. 7}$$

View Article Online
DOI: 10.1039/C8PY00829A

The enthalpy of mixing is then given as the product of the volume fractions and a constant of interaction, expressed here as the Flory parameter.[43,44] In the particle model only the surface area of the polymer can interact with the solvent, and so only this is included:

$$\Delta H_m = k_B T \phi_s A \chi_{s,p} \quad \text{Eq. 8}$$

Where ϕ_s is the volume fraction of the solvent, $(n_0 - Nx)/n_0$, and the total area of all polymer material A is given by Equation 9:

$$A = N\pi^{\frac{1}{3}}(6x)^{\frac{2}{3}} \quad \text{Eq. 9}$$

The expression for ΔH_m here is therefore equal to a constant of polymer unit–solvent interaction ($\chi_{s,p}$, here describing the interaction of the cell-cell interactions) scaled according to the rate of occurrence, accounting for the lack of interaction between solvent and polymer units within the polymeric sphere ($\chi_{s,p}$ between identical substances is defined as zero, as described previously). Combining these equations therefore gives a simple model for the Gibbs free energy of mixing:

$$\Delta G_m = k_B T \left[\phi_s A \chi_{s,p} + n \ln\left(\frac{n}{n_0}\right) + N \ln\left(\frac{xN}{v}\right)\right] \quad \text{Eq. 10}$$

For these calculations it will be assumed that the conversion of monomer to polymer is 100 % and that the volume fraction occupied by the polymer is equal to that occupied by the reagents.

Spinodal and binodal phase separation

The relationship described between $\chi_{s,p}$ and particle diameter is also dependent on a minimal value for $\chi_{s,p}$ for successful synthesis. Empirical investigation combined with the thermodynamic model outlined previously gives some insight into the basis of this minimal $\chi_{s,p}$, by approximating ΔG_m values and thus predicting phase separation behavior. Phase separation from polymer solutions may occur by either nucleation and growth, if the system is meta-stable, or spinodal decomposition if the system is unstable.[45] In a system of two miscible components, the spinodal is typically defined by the condition below, in terms of the volume fraction ϕ_p, where $\phi_p = xN/\underline{n}_0$:[46,47]

$$\left(\frac{\partial^2 \Delta G_m}{\partial \phi_p^2}\right)_{P,T} = \left(\frac{\partial^2 \Delta G_m}{\partial \left(\frac{xN}{n_0}\right)^2}\right)_{P,T} = 0 \quad \text{Eq. 11}$$

This inflection represents the point of spontaneous phase separation or spinodal decomposition, as the homogenous mixture reaches its limit of stability. The spinodal or spinodal curve can be observed relatively easy as it is the point beyond which a homogeneous phase will separate into two distinct phases, and in the case of polymer nanoparticle synthesis, precipitation occurs. Small droplets of polymer spontaneously separate from the solvent throughout the system, acting as nucleation sites, and the polymers are grown from the solution.[48] At higher concentrations spinodal decomposition produces membrane-like structures, the individual fibers of which rapidly expand to reduce the surface area of the new phase.[44]

The full spinodal is typically determined by measuring the tangent points at various temperatures, the combination of which gives the spinodal curve. Observation of different values of calculated $\chi_{s,p}$ are however practically equivalent to observation of different temperatures, and are also commonly used.[37,49] Phase separation will occur for any value of ϕ_p between the tangent points, above the low-ϕ_p ΔG_m minimum and the high-ϕ_p, ΔG_m minimum.[37] Below a particular value of $\chi_{s,p}$ no local low-ϕ_p is present (i.e. the affinity for the solvent is sufficiently high) and no separation occurs. As $\chi_{s,p}$ is reduced the tangents point become closer until they meet at the critical temperature (T_c) or critical Flory parameter (χ_c), representing the critical point.

Under conditions other those of the critical point, the spinodal represents the boundary between that of phase separation and a region of homogeneous metastability. The metastable region is found beyond the point of equilibrium, the function referred to as the binodal, described by Equation 12:[44]

$$\left(\frac{\partial \Delta G_m\left(\frac{xN}{n_0}\right)'}{\partial\left(\frac{xN}{n_0}\right)}\right)_{P,T} = \left(\frac{\partial \Delta G_m\left(\frac{xN}{n_0}\right)''}{\partial\left(\frac{xN}{n_0}\right)}\right)_{P,T} \quad \text{Eq. 12}$$

Where prime and double prime refer to the two phases of the mixture, the binodal thus representing the point of equilibrium between two phases as a typical phase diagram, while the spinodal shows the limit of stability. At χ_c, the binodal and spinodal are equivalent, and the point at which the second phase is favored is the same as that at which the existing system becomes unstable.

Phase separation from a homogeneous system in the metastable region beyond the binodal requires spontaneous phase separation of small droplets, followed by their growth by diffusion. The growth of the droplets proceeds readily by diffusion as the equilibrium point (Equation 12), i.e. the binodal has already been passed, but the point of stability (Equation 11), the spinodal, has not.[47] In the metastable state therefore, an energy barrier to phase separation must be overcome in order to induce precipitation from a homogeneous mixture, and in the event of such phase separation being induced, the resulting particles are formed extremely slowly and with high polydispersity.[44] In addition to this, random phase separation from a homogeneous mixture is associated with a quantity of work proportional to the volume of the new phase, with a minimum size requirement for energetically favorable development of the emerging phase.[50]

In a nucleated systems however, phase separation occurs via the equilibration of the growing polymers with the existing nucleant separate phase. As the early polymer develops the character of the MSPU, the affinity of the oligomers for the solvent decreases as it approaches $\chi_{s,p}$. In the presence of a suitable nucleant the equilibrium between the solvated state and complexed state shifts as the reaction proceeds, the equilibrium point between these being the binodal. Beyond the binodal in the metastable region, the nucleant is favored as a local fluctuation in ΔG_m and polymerization proceeds from

View Article Online
DOI: 10.1039/C8PY00829A

these sites. The specific system used in the experiments described was designed in such a way that the monomer would interact strongly with the nucleant, encouraging early binodal phase separation.

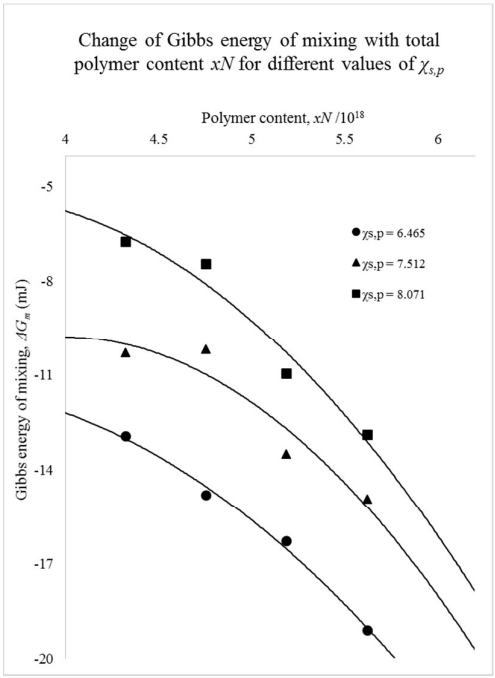

Fig. 1 Gibbs energy of mixing over several polymer fractions with different Flory parameters; $\partial\Delta G_m/\partial xN$ is observed to increase with greater $\chi_{s,p}$ as the lower approaches the inflection.

Figure 1 demonstrates the relationship between ΔG_m and $\chi_{s,p}$ over a short range of xN, the lower value of χs,p giving a reduced $\partial\Delta G_m/\partial xN$ as the inflection point spinodal is approached for polymers synthesized in the absence of nucleant. At the peak of each ΔG_m curve polymer synthesis was unsuccessful, as would be expected from reaching the spinodal. The coordinate $\chi_{s,p}$ = 5.821: $xN = 3.026 \times 10^{18}$ is a suspected spinodal phase boundary based on success in polymerization at all greater values of $\chi_{s,p}$ at the given xN, and greater xN at the given $\chi_{s,p}$, with consistent failure in polymerization with lower values; low concentrations of polydisperse polymer was found at the boundary. Due to the binodal being below the spinodal, polymers were formed in the presence of a nucleant at values of $\chi_{s,p}$ below those where unnucleated synthesis was unsuccessful.

The mechanisms required for system transition from single phase to two phases across the spinodal are different to those occurring during phase separation in the metastable region beyond the binodal, the mechanisms of the latter resembling those of crystallization.[43] This is an important addition as it suggests that polymers formed in the presence of a nucleant are fundamentally different from those without, and that regular arrangements representing the most energetically favorable interactions of monomers or oligomers around the seed compound may be found in the former. In the absence of detailed analysis of many different polymeric systems however this remains speculative. In the next section the practical value of finding the spinodal and binodal will be addressed.

The predictive capacity of Δχ

The spinodal and binodal on a $\chi_{s,p}(xN)$ plot represents the minimal $\chi_{s,p}$ required to induce phase separation at a given value of xN (total polymer content). The spinodal $\chi_{s,p}$ (from here $\chi_{spinodal}$) is that required for spinodal character phase separation (unnucleated polymerization), and the binodal $\chi_{s,p}$ ($\chi_{binodal}$) that required for binodal character phase separation (nucleated polymerization).

As previously discussed, $\chi_{spinodal}$ was determined to be approximately 5.8 at $xN = 3.026 \times 10^{18}$. Unsuccessful polymerization at $xN = 4.323 \times 10^{18}$ (standard) with $\chi_{s,p}$ = 5.131 suggests that this value of xN, $\chi_{spinodal}$ is approximately 5.5. Taking this, a term $\Delta\chi_{spinodal} = \chi_{s,p} - \chi_{spinodal}$ can be calculated, and a plot vs. nanoparticle hydrodynamic diameter gives an approximately linear relationship D(nm) = $-74\Delta\chi_{spinodal}$ + 367 nm (Figure 2).

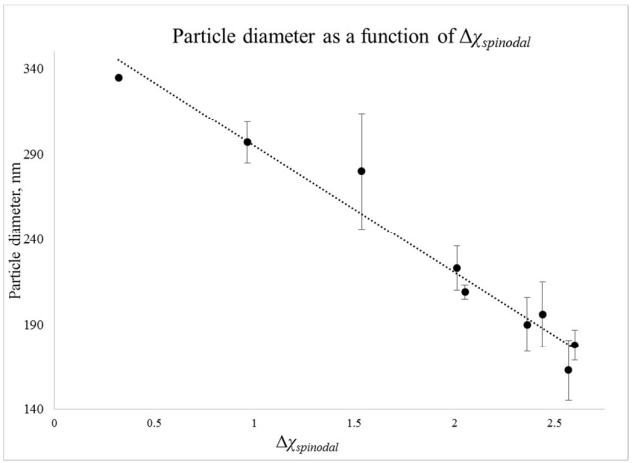

Fig. 2 The relationship between particle hydrodynamic diameter and $\Delta\chi_{spinodal}$, where $\Delta\chi_{spinodal} = \chi_{s,p} - \chi_{spinodal}$. At this xN, D(nm) = $-74\Delta\chi_{spinodal}$ + 367 nm.

Repetition with alternative solvent validates this equation as a general trend at the given value of xN: water-methanol systems equivalent to $\Delta\chi_{spinodal}$ 1.965 (235 nm (predicted 222 nm)) and 1.721 (260 nm (predicted 240 nm)) demonstrating relatively good correlation despite problems often encountered with methanol in polymer synthesis. Successful spinodal-character polymerization also requires $\Delta\chi_{spinodal}$ to be greater than zero, but the relationship given will be erased by the presence of nucleants, due the equivalent $\Delta\chi_{binodal}$ then being dominant. This was demonstrated by successful polymerization in the presence of a streptomycin nucleant at a $\Delta\chi_{spinodal}$ value of -1.083, far below the value where unnucleated attempts were successful (Appendix 2). An overview of the model is given in Figure 3 and the Table of Contents graphic.

View Article Online
DOI: 10.1039/C8PY00829A

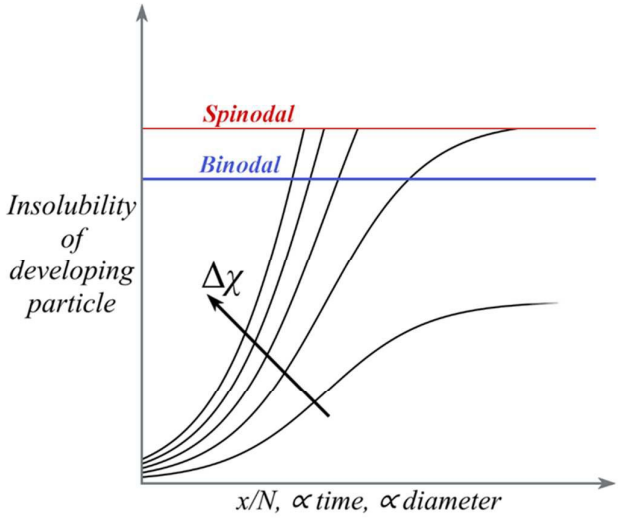

Fig. 3 Insolubility of developing particle over time, x/N and final particle diameter. The particle grows until it reaches $\chi_{s,p}$, the plateau of the sigmoid curve of insolubility. Separation occurs at the spinodal or from the binodal. The shape of the sigmoid curve, and thus the nanoparticle diameter, depends on $\Delta\chi$ (the position of $\chi_{s,p}$ relative to the spinodal or binodal) .

The equation given above for $\Delta\chi_{spinodal}$ however will not hold for values of xN other than that given (4.323×10^{18}). Simple analysis with the data collected previously with variation in xN for analysis of the Gibbs energy however gives a possible relationship. With the assumption that the trend in $\chi_{spinodal}$ continues linearly as it does from $xN = 3.026 \times 10^{18}$ to $xN = 4.323 \times 10^{18}$, through to $xN = 5.620 \times 10^{18}$, the plot of particle hydrodynamic diameter as a function of $(xN)^2/\Delta\chi_{spinodal}$ is given in Figure 4; the trend shown can be approximated to D(nm) = $173\ln[(xN)^2 10^{-36}/\Delta\chi_{spinodal}] - 193$ nm.

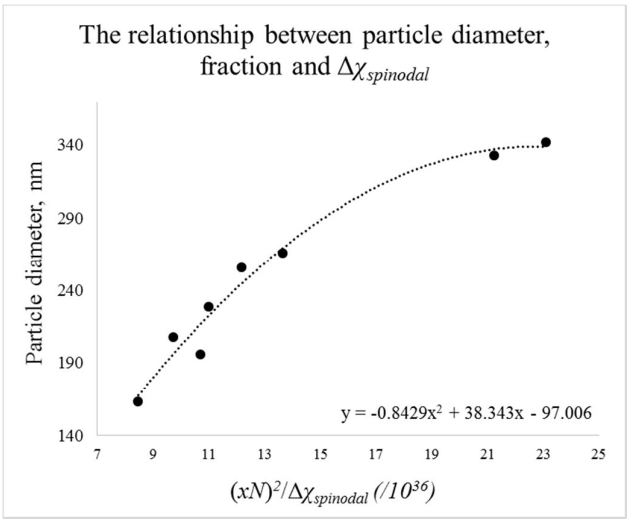

Fig. 4 The relationship between particle diameter, fraction (expressed in values of xN) and $\Delta\chi_{spinodal}$. The trend line shown is given by the equation in the Figure, but can be approximated to D(nm) = $173\ln[(xN)^2 10^{-36}/\Delta\chi_{spinodal}] - 193$ nm.

Further experiments are required however to fully determine the relationship beyond the relatively narrow range within which xN was varied. An additional point of further work centers on $\Delta\chi_{binodal}$. While inducing binodal-character phase separation of polymer nanoparticles is relatively simple by comparison (indeed often difficult to avoid entirely due the presence of contaminant) due to the lower value of $\chi_{binodal}$ permitting a wider range of reaction conditions, generating relevant experimental data that helps with producing any consistent model of binodal-character phase separation will inherently be much more difficult than that associated with the spinodal. As Equation 12 shows, the position of the binodal is dependent on the relative affinity of the MSPU for the nucleant and the solvent. The relationship between polymer and solvent given by $\chi_{s,p}$ then becomes irrelevant unless it is accompanied by an additional term expressing the interaction between polymer and nucleant, a relationship which can less easily be expressed with typical solubility parameters. Additionally, as the nucleant acts as a local fluctuation in the Gibbs energy in the profile of the system which the developing polymer may adsorb into, the solubility of the nucleant will also need to be included in any effective model of binodal-character phase separation.

Conclusions

The relationship between polymer nanoparticle diameter and solubility has been established for phase separation at the spinodal in unnucleated particles, being dependent on the value of $\Delta\chi_{spinodal}$. Increasing values of $\Delta\chi_{spinodal}$ correlate with decreasing particle dimensions for $\Delta\chi_{spinodal}$ greater than zero. Within some range this trend can also be extended to different polymer fractions, correlating with $(xN)^2/\Delta\chi_{spinodal}$. As control of nanoparticle dimensions is essential for applications in vivo this model should prove very useful to researchers in the field. Particle synthesis with $\Delta\chi_{spinodal} < 0$ is associated with nucleated separation within the metastable region between the binodal and spinodal. The synthetic mechanisms of binodal character and spinodal character separation are therefore largely incomparable and further analysis of the equivalent $\Delta\chi_{binodal}$ is required, the regularity of the nucleated particle core and total size being dependent on monomer/polymer-nucleant interactions beyond the equilibrium binodal. Further studies with electron microscopy are also required to analyse the shape of the nanoparticles and corroborate the observed relationships in size. To the best of our knowledge however this is the first successful Flory-Huggins based thermodynamic model of polymer nanoparticles, and should provide a useful guide to predictive design of future nanomaterials.

Conflicts of interest

There are no conflicts to declare

View Article Online
DOI: 10.1039/C8PY00829A

Acknowledgements

With thanks to Joanna Czulak, Antonio Guerreiro, Alistair Watson and Matthew Young.

References

1. A. F. M. Barton, *Chemical Reviews*, 1975, **75**, 731-753.
2. D. J. Greenhalgh, A. C. Williams, P. Timmins and P. York, *J. Pharm. Sci.*, 1999, **88**, 1182-1190.
3. R. F. Fedors, *Polymer Engineering & Science*, 1974, **14**, 147-154.
4. B. C. Hancock, P. York and R. C. Rowe, *Int. J. Pharm.*, 1997, **148**, 1-21.
5. G. DiPaola-Baranyi and J. E. Guillet, *Macromolecules*, 1978, **11**, 228-235.
6. Y. Zhu and L. Liao, *Journal of Nanoscience and Nanotechnology*, 2015, **15**, 4753-4773.
7. H. Meng, M. Liong, T. Xia, Z. Li, Z. Ji, J. I. Zink and A. E. Nel, *ACS Nano*, 2010, **4**, 4539-4550.
8. S. K. Sahoo and V. Labhasetwar, *Molecular Pharmaceutics*, 2005, **2**, 373-383.
9. S. A. A. Rizvi and A. M. Saleh, *Saudi Pharmaceutical Journal*, 2018, **26**, 64-70.
10. E. Pérez-Herrero and A. Fernández-Medarde, *European Journal of Pharmaceutics and Biopharmaceutics*, 2015, **93**, 52-79.
11. K. Ulbrich, K. Holá, V. Šubr, A. Bakandritsos, J. Tuček and R. Zbořil, *Chemical Reviews*, 2016, **116**, 5338-5431.
12. C. Wu, B. Bull, C. Szymanski, K. Christensen and J. McNeill, *ACS Nano*, 2008, **2**, 2415-2423.
13. A. A. Shemetov, I. Nabiev and A. Sukhanova, *ACS Nano*, 2012, **6**, 4585-4602.
14. X. Yu, I. Trase, M. Ren, K. Duval, X. Guo and Z. Chen, *Journal of Nanomaterials*, 2016, **2016**, 15.
15. J. J. Shi, P. W. Kantoff, R. Wooster and O. C. Farokhzad, *Nat. Rev. Cancer*, 2017, **17**, 20-37.
16. J. M. Rosenholm, A. Meinander, E. Peuhu, R. Niemi, J. E. Eriksson, C. Sahlgren and M. Lindén, *ACS Nano*, 2009, **3**, 197-206.
17. M. P. Desai, V. Labhasetwar, E. Walter, R. J. Levy and G. L. Amidon, *Pharm. Res.*, 1997, **14**, 1568-1573.
18. H. Gao, W. Shi and L. B. Freund, *Proc. Natl. Acad. Sci. U. S. A.*, 2005, **102**, 9469-9474.
19. B. D. Chithrani and W. C. W. Chan, *Nano Letters*, 2007, **7**, 1542-1550.
20. B. D. Chithrani, A. A. Ghazani and W. C. W. Chan, *Nano Letters*, 2006, **6**, 662-668.
21. F. Osaki, T. Kanamori, S. Sando, T. Sera and Y. Aoyama, *J Am. Chem. Soc.*, 2004, **126**, 6520-6521.
22. W.-K. Oh, S. Kim, M. Choi, C. Kim, Y. S. Jeong, B.-R. Cho, J.-S. Hahn and J. Jang, *ACS Nano*, 2010, **4**, 5301-5313.
23. J. M. Caster, S. K. Yu, A. N. Patel, N. J. Newman, Z. J. Lee, S. B. Warner, K. T. Wagner, K. C. Roche, X. Tian, Y. Z. Min and A. Z. Wang, *Nanomed.-Nanotechnol. Biol. Med.*, 2017, **13**, 1673-1683.
24. A. Prokop and J. M. Davidson, *J. Pharm. Sci.*, 2008, **97**, 3518-3590.
25. J. P. M. Almeida, A. L. Chen, A. Foster and R. Drezek, *Nanomedicine*, 2011, **6**, 815+.
26. S. Pardeshi, R. Dhodapkar and A. Kumar, *Food Chem.*, 2014, **146**, 385-393.
27. P. Hazot, T. Delair, C. Pichot, J.-P. Chapel and A. Elaissari, *Comptes Rendus Chimie*, 2003, **6**, 1417-1424.
28. B. Elmas, M. Tuncel, S. Şenel, S. Patir and A. Tuncel, *Journal of Colloid and Interface Science*, 2007, **313**, 174-183.
29. L. Yang, Z. Fan, T. Wang, W. Cai, M. Yang, P. Jiang, M. Zhang and X. Dong, *Anal. Lett.*, 2011, **44**, 2617-2632.
30. F. Canfarotta, A. Poma, A. Guerreiro and S. Piletsky, *Nat. Protoc.*, 2016, **11**, 443-455.
31. J. S. Downey, R. S. Frank, W.-H. Li and H. D. H. Stöver, *Macromolecules*, 1999, **32**, 2838-2844.
32. J. N. Nayak, M. I. Aralaguppi, B. V. Kumar Naidu and T. M. Aminabhavi, *Journal of Chemical & Engineering Data*, 2004, **49**, 468-474.
33. P. S. Albright and L. J. Gosting, *J Am. Chem. Soc.*, 1946, **68**, 1061-1063.
34. C. Carr and J. A. Riddick, *Industrial & Engineering Chemistry*, 1951, **43**, 692-696.
35. J. V. Herráez and R. Belda, *Journal of Solution Chemistry*, 2006, **35**, 1315-1328.
36. A. L. Medina-Castillo, J. F. Fernandez-Sanchez, A. Segura-Carretero and A. Fernandez-Gutierrez, *Macromolecules*, 2010, **43**, 5804-5813.
37. D. W. Van Krevelen and K. Te Nijenhuis, in *Properties of Polymers (Fourth Edition)*, Elsevier, Amsterdam, Editon edn., 2009, pp. 189-227.
38. E. A. Grulke, in *Polymer Handbook*, eds. J. Brandrup, E. H. Immergut and E. A. Grulke, John Wiley & Sons, inc., New York, USA, Editon edn., 1999, vol. Four, p. VII.
39. C. M. Hansen, *Hansen Solubility Parameters: A User's Handbook*, second edn., CRC Press, Boca Raton, FL, 2007.
40. Y. Hoshino, T. Urakami, T. Kodama, H. Koide, N. Oku, Y. Okahata and K. J. Shea, *Small*, 2009, **5**, 1562-1568.
41. Y. Hoshino, H. Koide, T. Urakami, H. Kanazawa, T. Kodama, N. Oku and K. J. Shea, *J. Am. Chem. Soc.*, 2010, **132**, 6644-+.
42. P. J. Flory, *The Journal of Chemical Physics*, 1942, **10**, 51-61.
43. E. Manias and L. A. Utracki, in *Polymer Blends Handbook*, eds. L. A. Utracki and C. A. Wilkie, Springer Netherlands, Dordrecht, Editon edn., 2014, pp. 171-289.
44. F. S. Bates, *Science*, 1991, **251**, 898-905.
45. E. P. Favvas and A. C. Mitropoulos, *J. Eng. Sci. Tech. Rev.*, 2008, **1**, 25-27.
46. B. Grosdidier, S. M. Osman and A. Ben Abdellah, *Physical Review B*, 2008, **78**, 024205.
47. N. P. Young and N. P. Balsara, in *Encyclopedia of Polymeric Nanomaterials*, eds. S. Kobayashi and K. Müllen, Springer Berlin, Heidelberg, Editon edn., 2015, pp. 777-782.
48. N. P. Young and N. P. Balsara, in *Encyclopedia of Polymeric Nanomaterials*, eds. S. Kobayashi and K. Müllen, Springer Berlin, Heidelberg, Editon edn., 2015, pp. 747-755.
49. T. Ougizawa and T. Inoue, *Polym J*, 1986, **18**, 521-527.
50. D. Kashchiev, *Nucleation : Basic Theory with Applications*, Elsevier Science, Oxford, 2000.

View Article Online
DOI: 10.1039/C8PY00829A

The application of Flory-Huggins theory for the prediction and control of polymer nanoparticle dimensions